Asia-Pacific Magnetic Recording Conference 2018
15 - 17 November 2018, USST, China

Mixed H_2/H_∞ Data-Driven Control Design for Hard Disk Drives

Omid Baghereih[1] and Roberto Horowitz[1]
[1]Department of Mechanical Engineering, University of California, Berkeley, CA 94720 USA

A frequency based data-driven control design considering mixed H_2/H_∞ control objectives is developed for multiple input-single output systems. The main advantage of the data-driven control over the model-based control is its ability to use the frequency response measurements of the controlled plant directly without the need to identify a model for the plant. In the proposed methodology, multiple sets of measurements can be considered in the design process to accommodate variations in the system dynamics. The controller is obtained by translating the mixed H_2/H_∞ control objectives into a convex optimization problem. The H_∞ norm is used to shape closed loop transfer functions and guarantee closed loop stability, while the H_2 norm is used to constrain and/or minimize the variance of signals in the time domain. The proposed data-driven design methodology is used to design a track following controller for a dual-stage Hard Disk Drive (HDD), based on the sensitivity decoupling structure.

***Index Terms*—Data-driven control design, Mixed H_2/H_∞ norms, Multiple input-single output systems, Hard disk drives, Track-following controller, Sensitivity decoupling.**

I. Introduction

Control systems for the dual-stage actuators in HDDs have been designed using a variety of model-based design techniques. In this paper we will however explore the use of data-driven control design methodologies, which only utilized frequency response data [2], [4], [5]. Specifically, we consider the design of track-following servo systems for dual-stage HDDs using mixed H_2/H_∞ data driven synthesis techniques. The proposed algorithm combines the necessary and sufficient convex conditions for the H_∞ norm for Multi-Input Single-Output (MISO) plants [1] with sufficient convex conditions for the H_2 norm [4]. Dual-stage actuators in HDDs normally accept two control inputs, while having only one measurement output. Therefore, the controller for this system will be a single input-multi output controller (SIMO). Frequent practice in the HDD industry is to decouple the dual-stage system into two SISO systems using the well-known methodology sensitivity decoupling approach [6], [3]. We will use the sensitivity decoupling approach to design compensators for dual-stage actuators in two sequential steps by considering the mixed H_2/H_∞ design process for SISO systems and will refer to this approach as the *Sequential SISO design strategy*. We will also utilize the mixed H_2/H_∞ synthesis methodology developed for SIMO controllers, to simultaneously design both of the compensators in a sensitivity decoupling control architecture, and will referred to this approach as the *SIMO design strategy*. Control systems designed using these two strategies will be evaluated, and their performance compared.

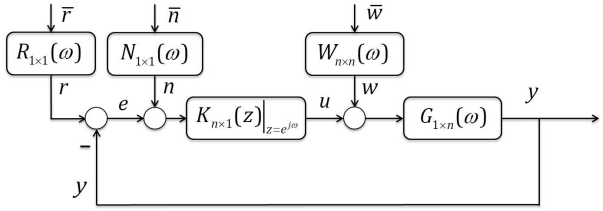

Fig. 1: Control block diagram. $G(\omega)$ represents the frequency response data of the plant. The disturbances to the system are colored by the stable weighting functions $R(\omega) \in \mathbb{RH}_\infty$, $N(\omega) \in \mathbb{RH}_\infty$ and $W(\omega) \in \mathbb{RH}_\infty^{n\times n}$.

II. Preliminaries

$G(z)$ and $G(e^{j\omega})$ respectively represent discrete-time transfer functions in the z and frequency domains. $\mathbb{R}_{p,q}^{m\times n} \subset \mathbb{R}_p^{m\times n}$ is formed by all rational causal transfer functions with n inputs and m outputs of order q. $\mathbb{RH}_\infty^{m\times n}$ denotes the class of all asymptotically stable rational proper transfer functions with m outputs and n inputs. We will consider transfer functions that are only characterized by their frequency domain data, and do not have an *explicit model* representation and will use the argument $G(\omega)$ to represent them. We also make extensive use of H_∞ and H_2 norms

Consider the stable feedback system in Fig. 1, The well-known stable factorization results [7] will be used to factorize the plant and controller for these systems.

$$G(\omega) = \tilde{M}^{-1}(\omega)\tilde{N}(\omega),\ \tilde{M} \in \mathbb{RH}_\infty,\ \tilde{N} \in \mathbb{RH}_\infty^{1\times n} \quad (1)$$

$$K(z) = X(z)Y^{-1}(z),\quad Y \in \mathbb{RH}_\infty,\ X \in \mathbb{RH}_\infty^{n\times 1} \quad (2)$$

The feedback structure given in Fig. 1 will be used to design the controller $K(z)$. Signals $\bar{r}, \bar{n}, \bar{w}$ are zero-mean white noises with unit variances, and the filter blocks $R \in \mathbb{RH}_\infty$, $N \in \mathbb{RH}_\infty$, $W \in \mathbb{RH}_\infty^{n\times n}$ are used to color these noises. The sequence $e = (r - y)$ is often referred to as the *position error signal (PES)*. (1) and (2) can be used to derive the closed loop transfer functions from external signals in Fig. 1 to the tracking error e, the control input u and the measurement output y respectively, in terms of the stable factorizations.

$$\begin{bmatrix} E_r & E_n & E_w \\ U_r & U_n & U_w \\ Y_r & Y_n & Y_w \end{bmatrix} = \frac{1}{\tilde{N}X + \tilde{M}Y} \begin{bmatrix} \tilde{M}Y & -\tilde{M}Y & -\tilde{N}Y \\ \tilde{M}X & \tilde{M}X & -X\tilde{N} \\ \tilde{N}X & \tilde{N}X & \tilde{N}Y \end{bmatrix} \quad (3)$$

In (3) E_r denotes the closed loop transfer function from input r to output e, U_w denotes the the closed loop transfer function from input w to output u, and so on. All functions in (3) have

the same closed loop poles, which are the roots of $\tilde{N}X + \tilde{M}Y \in \mathbb{RH}_\infty$.

In this paper we will assume that there are l frequency response measurements available for the plant G in Fig. 1, and will denote the i's measurement by $G_i(\omega)$. Similarly, $E_{r,i}$, $U_{w,i}$ and $Y_{r,i}$ are the closed loop transfer functions for the i^{th} frequency domain data set.

III. Control Synthesis Algorithms

In [5], *Karimi et al.* proposed a data-driven H_∞ control design methodology for SISO plants. In this paper, we present an extension to Multi-Input and Single-Output (MISO) plants [1]. The convex condition for the H_∞ norm of the closed loop transfer function from control input disturbance w to control input u, $U_{w,i} \in \mathbb{R}_p^{n\times n}$ in (3) is presented. The procedure for obtaining the convex condition of all other closed loop transfer functions in (3) is similar.

Theorem III.1. *Assume that the frequency response data for the i^{th} measurement of the plant, $G_i(\omega) \in \mathbb{R}_p^{1\times n}$, is given over the frequency region Ω, and is factorized according to Eq. (1). Given positive scalars γ, the following two statements are equivalent.*

- *I) Controller $K(z)$ stabilizes the plant $G_i(\omega)$ and*

$$\|W_{U_w} U_{w,i}\|_\infty < \gamma, \ \forall\, i \in \{1, \cdots, l\}\,. \tag{4}$$

  where W_{U_w} is a frequency weighting function.
- *II) There exists controller stable controller factorizations $X(z) \in \mathbb{RH}_\infty^{n\times 1}$ and $Y(z) \in \mathbb{RH}_\infty$, such that the following convex inequality holds $\forall i \in \{1, \cdots, l\}$ and $\forall \omega \in \Omega$*

$$\gamma^{-1}\bar{\sigma}(\ W_{U_w}(\omega)X(e^{j\omega})\tilde{N}_i(\omega)\ ) < Re(\ \tilde{N}_i(\omega)X(e^{j\omega}) + \tilde{M}_i(\omega)Y(e^{j\omega})\ )\,. \tag{5}$$

  where $\bar{\sigma}(\cdot)$ is the maximum singular value and $Re(\cdot)$ is the real part.

Proof: [1].

Consider again the MISO system given in Fig. 1 and assume, that the exogenous sequences, $\bar{r}$, $\bar{n}$ and $\bar{w}$ are zero-mean independent white noises with unit variances. A key design objecting for track-following controllers of HDDs is to minimize the variance of the position error signal (PES). Therefore, in this paper we will consider the minimization of the average variance of the error sequence $e = r - y$, for all l frequency domain data sets.

$$\frac{1}{l}\sum_{i=1}^{l} ||e_i||_2^2 = \frac{1}{l}\sum_{i=1}^{l}\left[||E_{r,i}R||_2^2 + ||E_{n,i}N||_2^2 + ||E_{w,i}W||_2^2\right] \tag{6}$$

where the frequency weights $R(\omega)$, $W(\omega)$ and $N(\omega)$ characterize the colored exogenous random disturbance inputs. It is also possible to constrain the *worst* variance of some sequences of all l frequency responses of the plant, for example the worst case variance of the control input, $||u_i||_2^2 \le \beta_u$ for some $\beta_u > 0$ and for all $i = 1, \cdots l$; or constrain the *average* variance, of the control input, $\frac{1}{l}\sum_{i=1}^{l} ||u_i||_2^2 \le \beta_u$, given l frequency responses.

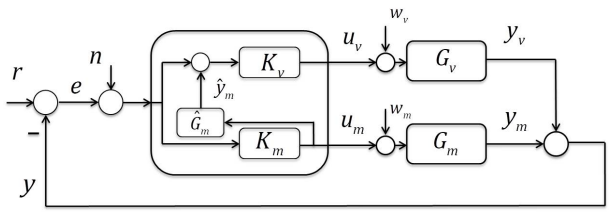

Fig. 2: Sensitivity decoupling control Structure for a dual-stage HDD. $\hat{G}_m(z)$ represents an estimated Mili-Actuator (MA) transfer function. In order to switch to the single-stage HDD with VCM as the actuator also known as the single-stage VCM loop, signals u_m and $\hat{y}_m$ are set to zero.

We will use results from [4] is used to determine an upper bound to H_2 norms.

The H_2 and H_∞ criteria can be combined to form a mixed H_2/H_∞ control design problem. The sufficient convex conditions for the H_2 norm criteria in [4] are used to impose the H_2 norm constraints or minimization objectives. The necessary and sufficient H_∞ convex conditions in theorem III.1 [1] guarantee closed loop stability and are used for loop shaping.

IV. HDD Track Following Design Results

A Voice Coil Motor (VCM) and a PZT Mili-Actuator (MA) are the most frequently used actuators for nano-positioning the head on the data tracks in HDDs. These two actuators are respectively denoted as G_v and G_m in the dual-stage feedback structure shown in Fig. 2. Four sources of external noises and/or disturbances are considered. r is the non-repeatable track run-out. Measurement noise n contaminates the position error signal, e, as measured by the magnetic read head. w_v and w_m are the control input sources respectively acting on the VCM head assembly and on the MA. The most commonly used control structure in dual-stage HDDs is the Sensitivity Decoupling structure illustrated in Fig. 2

Five sets of frequency response data are used to represent dynamics variations for each actuator (i.e. $l = 5$). These five sets of frequency response data are plotted in Fig. 3. Only the frequency response data generated by these transfer functions, in the form of factorizations $\tilde{N}_{v,i}(\omega)$, $\tilde{M}_{v,i}(\omega)$ and $\tilde{N}_{m,i}(\omega)$, $\tilde{M}_{m,i}(\omega)$, were used in the control synthesis algorithms, where i denotes the i^{th} frequency response of the $l = 5$ data set.

The compensators in the sensitivity decoupling structure given in Fig. 2 were designed under four different scenarios each involving a different value of η_{y_m}, the upper-limit of the square of the MA output stroke average variance.

$$\frac{1}{l}\sum_{i=1}^{l} \|y_{mi}\|_2^2 \le \eta_{y_m}, \tag{7}$$

where y_{mi} is the MA closed loop output in Fig. 2 for the i^{th} frequency response data. These values are shown in Table I, which presents the five cases of controller design scenarios that will be evaluated, as well as their respective marker type used in the plots. The data based synthesis methodology is an iterative approach. In this paper, all the controllers were synthesized using 10 iterations.

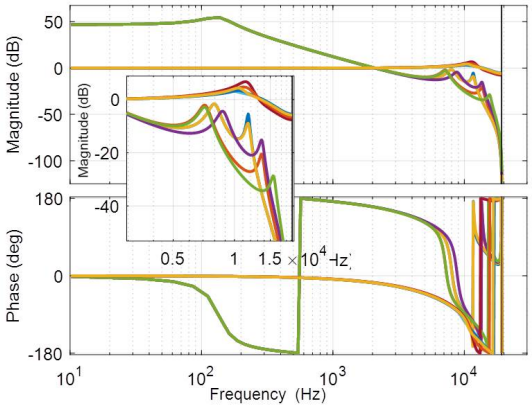

Fig. 3: Hard disk drive actuators frequency response measurement data sets used in the design. Five measurements from each actuator are used in the design. G_v and G_m represent VCM and MA actuators' transfer functions. The actuators output units for both the VCM and the MA are 10 nm.

TABLE I: Controller design scenarios and their marker type.

Index	Scenarios	Design strategies	η_{y_m} (nm^2)	Marker type
1	$SIMO_1$	SIMO	44^2	+
2	$SIMO_2$	SIMO	42^2	×
3	$SIMO_3$	SIMO	40^2	◁
4	$SIMO_4$	SIMO	38^2	▷
5	$SISO_1$	Sequential SISO	44^2	○

All closed loop transfer functions in the final, 10^{th} iteration, satisfied their respective H_∞ constraint limits.

Fig. 4a shows the magnitude Bode plot of the closed loop error rejection transfer function E_r, at the 10^{th} iteration, for the dual-stage feedback system in Fig. 2, and the five design scenarios described in for the five design scenarios described in table I. Also shown in the figure is the inverse of the weighting function $W_{E_r}(\omega)$, to space the closed loop error rejection sensitivity function E_r. Fig. 4b shows the the magnitude Bode plots of the closed loop transfer functions from the track runout *r* to the actuator outputs y_v and y_m respectively. As shown in the figure, the VCM is more active at the low frequency region, while the MA takes over at the mid-frequency region.

Since the z-domain transfer functions for all of the actuators frequency response measurements shown in Fig. 3 are available for this example, we were able to compute the closed loop poles of the feedback system, for all of the synthesized compensators and for all of the scenarios in table I, and to verify all the closed loop transfer functions were stable for all the plants used to generate the frequency response data in the data-driven mixed H_2/H_∞ formulation.

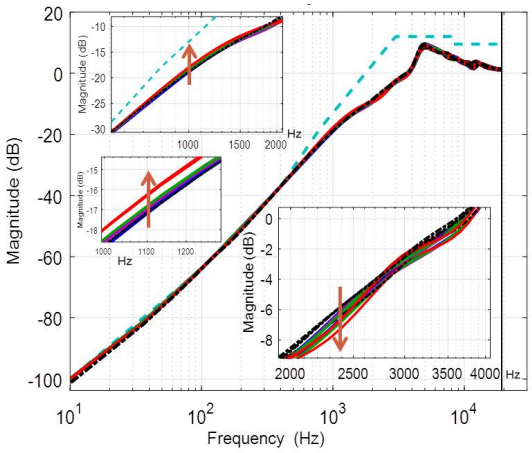

(a) E_r

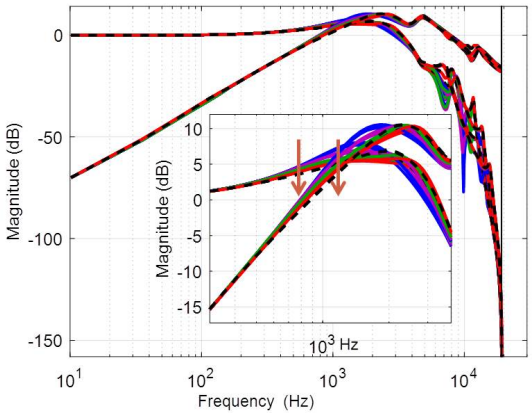

(b) Y_r^v and Y_r^m

Fig. 4: Magnitude Bode plots of the closed loop transfer functions: E_r (from track runout r to the tracking error e), Y_r^v (from r to VCM displacement y_v) and Y_r^m (from r to MA displacement y_v); for the dual-stage feedback loop in Fig. 2, after the 10^{th} iteration of the sequential SISO and the SIMO design strategies.These plots include 25 closed loop transfer functions for all the 5 design scenarios in table I using all the 5 frequency response data sets in Fig. 3. The arrows show the increasing direction for the scenario index numbers in table I.

ACKNOWLEDGMENT

This research was supported by the Western Digital Inc., the Advanced Storage Technology Committee (ASTC) and the UC Berkeley Computer Mechanics Laboratory (CML) sponsors.

REFERENCES

[1] Omid Baghereih, *Estimation, identification and data-driven control design for hard disk drives*, University of California, Berkeley, 2017.

[2] Gorka Galdos, Alireza Karimi, and Roland Longchamp, *H-infinity controller design for spectral mimo models by convex optimization*, Journal of Process Control **20** (2010), no. 10, 1175–1182.

[3] Roberto Horowitz, Yunfeng Li, Kenn Oldham, Stanley Kon, and Xinghui Huang, *Dual-stage servo systems and vibration compensation in computer hard disk drives*, Control Engineering Practice **15** (2007), no. 3, 291–305.

[4] A. Karimi and C. Kammer, *A data driven approach to robust control of multivariable systems by convex optimization*, Automatica.

[5] Alireza Karimi, Achille Nicoletti, and Yuanming Zhu, *Robust h-infinity controller design using frequency-domain data via convex optimization*, International Journal of Robust and Nonlinear Control (2016).

[6] K. Mori, T. Munemoto, H. Otsuki, Y. Yamaguchi, and K. Akagi, *A dual-stage magnetic disk drive actuator using a piezoelectric device for a high track density*, IEEE Trans. Magnetics **27** (1991), 5298–5300.

[7] TT Tay, JB Moore, and R Horowitz, *Indirect adaptive techniques for fixed controller performance enhancement*, International Journal of Control **50** (1989), no. 5, 1941–1959.